Liver sinusoidal endothelial cells constitute a major route for hemoglobin clearance

Gabriela Zurawska[1*], Zuzanna Sas[2*], Aneta Jończy[1], Patryk Slusarczyk[1], Raghunandan Mahadeva[1], Marta Chwałek[1], Maria Kulecka[3], Izabela Rumieńczyk[3], Morgane Moulin[4], Kamil Jastrzębski[1], Michal Mikula[3], Anders Etzerodt[4], Marta Miączyńska[1], Tomasz P. Rygiel[2,5,#,$] and Katarzyna Mleczko-Sanecka[1,#,$]

[1] International Institute of Molecular and Cell Biology in Warsaw, Warsaw, Poland

[2] Medical University of Warsaw, Warsaw, Poland

[3] Maria Sklodowska-Curie National Research Institute of Oncology, Warsaw, Poland

[4] Department of Biomedicine, Aarhus University, Aarhus, Denmark

[5] Mossakowski Medical Research Institute, Polish Academy of Sciences, Warsaw, Poland

*# equal contribution

$ To whom correspondence may be addressed: Katarzyna Mleczko-Sanecka, International Institute of Molecular and Cell Biology in Warsaw, 4 Ks. Trojdena Street, 02-109 Warsaw, Poland, E-mail: kmsanecka@iimcb.gov.pl

or

Tomasz P. Rygiel, Mossakowski Medical Research Institute, Polish Academy of Sciences, Warsaw, Poland, E-mail: t.rygiel@imdik.pan.pl

Key points:

- LSECs engage macropinocytosis to efficiently scavenge free hemoglobin
- LSEC-mediated hemoglobin clearance participates in iron recycling from spleen-derived hemoglobin and contributes to its detoxification during hemolysis

Abstract

Mild hemolysis of senescent erythrocytes occurs physiologically in the spleen, resulting in hemoglobin (Hb) release, whereas pathologic erythrocyte rupture characterizes several diseases. Iron recycling from Hb and Hb detoxification have been attributed to the sequestration of Hb-haptoglobin complexes by macrophages. However, we found the existence of additional efficient Hb clearance routes in mice. We identified liver sinusoidal endothelial cells (LSECs) as the primary cells responsible for Hb sequestration, a process that involves macropinocytosis and operates independently of the Hb-haptoglobin receptor CD163. LSECs expressed heme oxygenase 1 and hepcidin-controlled ferroportin and were the most efficient cellular scavengers of Hb at doses below and above the haptoglobin binding capacity. Erythrocyte transfusion assays further demonstrated that while splenic red pulp macrophages are adept at erytrophagocytosis, liver Kupffer cells and LSECs mainly clear erythrocyte ghosts and Hb, respectively, transported from the spleen via the portal circulation. High-dose Hb injections in mice resulted in transient hepatic iron retention and early activation of the gene encoding heme oxygenase 1 (*Hmox1*) in LSECs. This response was associated with the transcriptional induction of the iron-sensing angiokine *Bmp6*, culminating in hepcidin-mediated transient serum hypoferremia. Injection of Hb and iron citrate elicited distinct transcriptional signatures in LSECs, and the *Bmp6* induction was phenocopied by erythrocyte lysis upon phenylhydrazine. Collectively, we propose that LSECs provide a key mechanism for Hb clearance, a function that establishes the spleen-liver axis for physiological iron recycling from Hb and contributes to heme detoxification during hemolysis, coupled with the induction of the BMP6-hepcidin axis, ultimately restoring iron homeostasis.

Introduction

Internal iron recycling from senescent red blood cells (RBCs) satisfies most of the body's iron needs[1,2] and relies chiefly on phagocytic clearance of aged RBCs by the splenic red pulp macrophages (RPMs).[3,4] However, recent evidence suggests that some aged RBCs escape erythrophagocytosis and lyse locally in the spleen, thus releasing hemoglobin (Hb).[5] Several inherited and acquired disorders, including hereditary anemias, autoimmune hemolytic diseases, or infections, are characterized by compromised erythrocyte stability and increased risk of hemolysis.[6,7] Free Hb is captured by the acute phase plasma protein haptoglobin.[8] The Hb-haptoglobin complexes are sequestered via CD163,[9] a receptor that is highly expressed by both splenic RPMs and liver macrophages, Kupffer cells (KCs).[1,5] However, the role of these macrophage populations in Hb uptake has not been well characterized. Interestingly, pharmacokinetic studies in non-rodent mammals have shown that the clearance rate of the Hb-haptoglobin complex is significantly slower than that of free Hb,[10] and that Hb sequestration may occur independently of haptoglobin and/or CD163.[11,12] These observations are clinically relevant as enhanced erytrophagocytosis and prolonged erythrolytic conditions lead to the partial loss of the CD163-expressing iron-recycling macrophages[3,13] and are characterized by depletion of the plasma haptoglobin pool.[7,14,15] Collectively, this evidence suggests that macrophages may be dispensable for Hb clearance. It is well established that free Hb undergoes renal glomerular filtration.[16,17] However, it remains unclear whether other specialized routes of extra-renal and macrophage-independent Hb clearance operate in the body.

The liver receives approximately 25% of the cardiac output and is exposed to the blood from the portal circulation, which drains the gastrointestinal tract and the spleen.[18] The hepatic capillary network, composed of venous sinusoids, is specialized in monitoring and filtering the blood components. Liver sinusoidal endothelial cells (LSECs), along with KCs, confer the most efficient dual scavenging system in the body.[19] While KCs engulf large particles, LSECs remove macromolecules and nanoparticles, a function that protects the body from waste by-products and noxious blood factors.[20,21] The maintenance of appropriate iron homeostasis adds to the growing spectrum of homeostatic functions of LSECs. Importantly, LSECs are the sensors of body iron levels and the major producers of the inducible angiokine bone morphogenetic protein 6 (BMP6), and the homeostatic BMP2.[22,23] BMPs function as upstream activators of hepcidin, a key iron-regulatory hormone produced by liver hepatocytes. Hepcidin suppresses iron release into the bloodstream via the sole known iron exporter ferroportin (FPN), thereby limiting iron availability under iron-rich conditions.[24] However, it remains unclear how

different types of iron signals are sensed and detoxified in the liver microenvironment, and whether the emerging scavenging functions of LSECs cross-talk with their role in maintaining iron homeostasis. Here, we show that LSECs constitute a major route for Hb clearance. They contribute to steady-state iron recycling from spleen-derived Hb that enters the liver via the portal vein and participate in heme detoxification during hemolysis, timely coupled with the induction of the iron-sensing BMP6-hepcidin axis.

Results

LSECs engage macropinocytosis to sequester Hb

Studies using radiolabeled Hb showed that the clearance of injected hemoglobin is rapid[16] and mainly mediated by the liver, kidney, and spleen.[16,17] To address the involvement of macrophages in Hb uptake we first performed experiments using clodronate liposomes, a well-established strategy that depletes tissue macrophages, including hepatic KCs. Using a whole-organ imaging system, we observed that regardless of the KCs' presence, the liver emerged as the major organ sequestering fluorescently-labeled mouse Hb (Fig. 1A and S1). Using flow cytometry and confocal microscopy imaging, we next identified LSECs as the major hepatic cell type that takes up Hb, surpassing KCs, hepatocytes, and monocytes (Fig. 1B and C, see Data Supplements for gating strategies). To better understand the mechanism of Hb uptake we used primary cell cultures of NPCs, which fully recapitulated a higher capacity of LSECs than KCs in Hb uptake, as validated by confocal microscopy and flow cytometry (Fig. 1D and Fig. S2A). Interestingly, in contrast to KCs, LSECs were negative for the Hb-haptoglobin complex receptor, CD163 (Fig. 1E), and free Hb was taken up more robustly than the haptoglobin-bound Hb (Fig. 1F). We, therefore, hypothesized that LSECs may sequester Hb in a receptor-independent manner, possibly via macropinocytosis, a non-specific internalization of extracellular fluid.[26] Staining of primary LSECs with an early endosome marker, EEA1, identified many constitutively formed intracellular vesicles of macropinosome size (1-2 μm) (Fig. 1G and S2B). Fluorescently-labeled Hb was predominantly, though not exclusively, entrapped within such vesicles (Fig. 1G and S2B), and co-localized with high-molecular-weight dextran, a known macropinocytic cargo (Fig. 1H and S2C).[27,28] Consistently, a well-established blocker of macropinocytosis, ethylisopropyl amiloride (EIPA), in contrast to an inhibitor of clathrin-mediated endocytosis, chlorpromazine (CPZ), abolished Hb uptake (Fig. 1I and S2D). Likewise, Hb internalization was partially dependent on actin remodeling and Cdc42 activity, both important for macropinosome formation,[27] and canonical Wnt signaling via β-catenin, a pathway that is active in LSECs[29] and has previously been shown to activate macropinocytosis

(Fig. 1I).[30,31] Confirming the high macropinocytic capacity of LSECs *in vivo*, we demonstrated their ability for efficient uptake of fluorescently-labeled albumin, another known macropinocytic cargo (Fig. 1J).[28] Taken together, our data identify LSECs as efficient scavengers of both free and haptoglobin-bound Hb and implicate macropinocytosis as the pathway for Hb uptake.

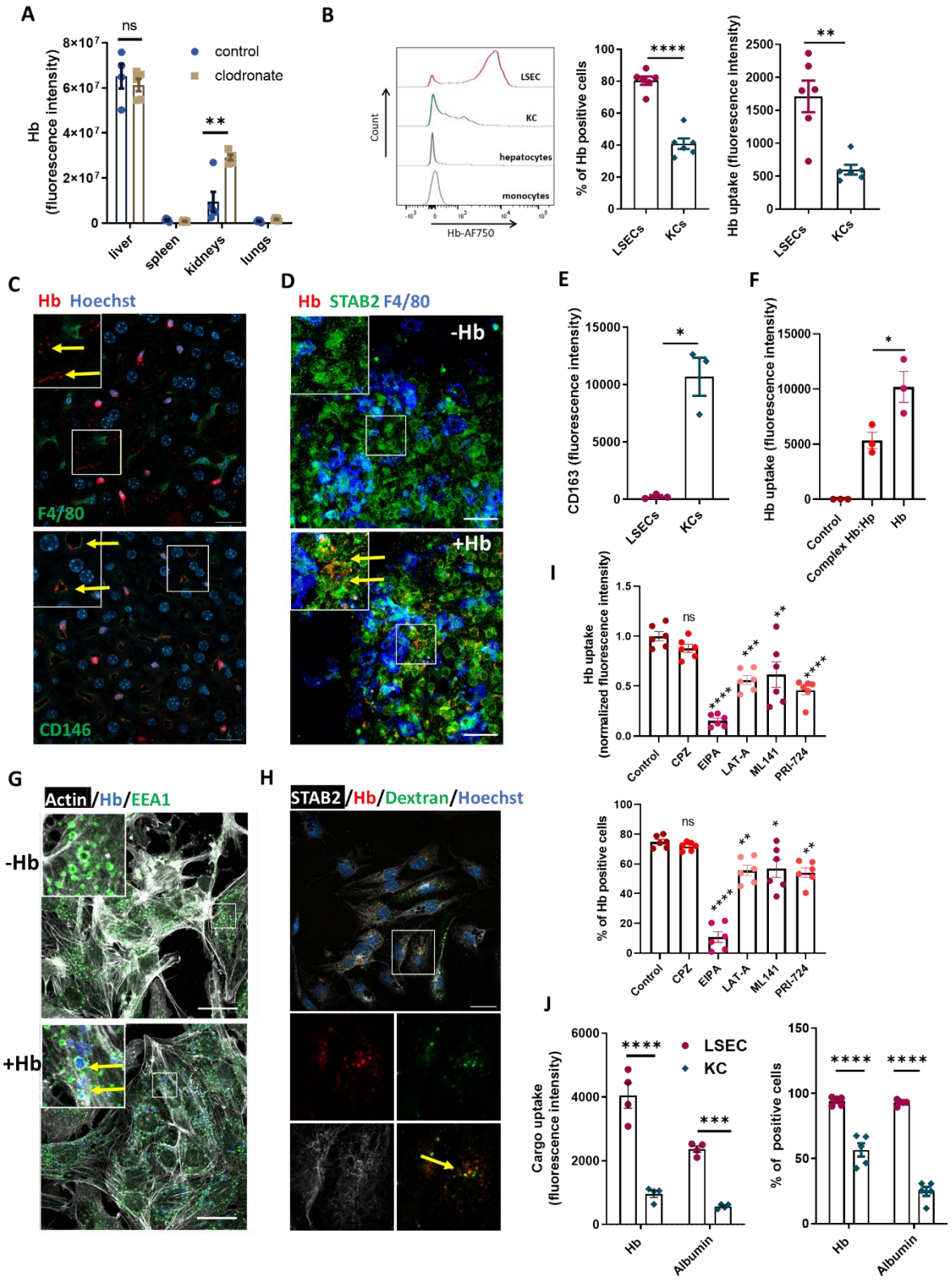

Figure 1. LSECs engage macropinocytosis to sequester Hb.

Hemoglobin (Hb) distribution in control and macrophage-depleted mice (clodronate) injected with Alexa Fluor 750-labeled Hb (Hb-AF750, 10 µg/mouse), imaged with Bruker *in vivo* Imaging System. Results are presented as total fluorescent counts from the region of interest. (B) AF750 fluorescence from particular liver cell populations isolated from Hb-AF750-injected mice was analyzed with flow cytometry. (C) Frozen liver slices from mice injected with Hb-AF647 (red) were processed and stained

for Kupffer cells (KCs) (F4/80, green) or LSECs (CD146, green) and nuclei (blue). Arrows indicate Hb presence in the LSEC. (D) Hb-AF750 uptake *in vitro* was imaged in liver nonparenchymal cells (NPCs) treated with Hb-AF750 (0.5 μg/ml) and stained for F4/80 (blue) and the LSEC marker STAB2 (green). Arrows indicate Hb-AF750 (red) presence in the LSEC. (C, D) - areas in the highlighted rectangles are shown at higher magnification (left upper corner), scale bars, 20 μm. (E) Cell-surface expression of the CD163 receptor on LSECs and KCs was measured by flow cytometry and presented as fluorescence intensity. (F) Uptake of Hb in the presence of haptoglobin, Hp [(Hb-AF750:Hp, 0.5 μg : 16 μg) /ml] in NPCs *in vitro* cultures was measured with flow cytometry. (G) Hb-AF647 vesicle localization was imaged with microscopy in NPCs *in vitro* cultures depleted from macrophages. Arrows indicate Hb-AF647 (blue) presence in the EEA-1$^+$ (green) and Actin$^+$ (white) vesicles. Areas in the highlighted rectangles are shown at higher magnification (left corner). Scale bars, 20 μm. (H) Co-localization of Hb-AF647 (red) with rhodamine-dextran (green) was imaged with microscopy in STAB2$^+$ LSECs (white). Arrow indicates colocalization of Hb and rhodamine-dextran. The area in the highlighted rectangle is shown at higher magnification in separate channels below. Scale bar, 20 μm. (I) NPCs were pre-treated with the clathrin-mediated endocytosis inhibitor chlorpromazine (CPZ), the macropinocytosis blocker EIPA, actin polymerization blocker latrunculin A (LAT-A), inhibitor of Cdc42 GTPase ML141, or with β-catenin inhibitor PRI-724 before Hb-AF750 treatment for 10 min. Flow cytometry was used to determine Hb uptake by the LSECs. (J) Mice were injected for 1 h with Hb-AF750 or albumin-AF750, both at 10 μg/mouse. The fluorescence intensity of AF750, the percentage of AF750$^+$ LSECs, and KCs populations were measured with flow cytometry. Microscopic images were acquired using confocal microscopes LSM 800 or LSM710 (Zeiss) equipped with an EC Plan-Neofluar 40x/1.30 or 63x/1.4 Oil DIC M27 oil objectives and T-PMT detectors and acquisition software ZEN 2.6/ZEN2009. The images were processed using ImageJ or Adobe Photoshop with linear gamma adjustments of contrast and brightness. Numerical data are expressed as mean ± SEM, each data point represents one biological replicate. Welch's unpaired t-test was used to determine statistical significance in B and E, one-way ANOVA with Tukey's Multiple Comparison tests was used in A, F, and J; while two-way ANOVA with Tukey's Multiple Comparison tests was used in I; ns - not significant, *p<0.05, **p<0.01, ***p<0.001 and ****p<0.0001

LSECs outperform other endothelial and macrophage populations in Hb uptake

Similar to the liver, sinusoidal endothelial cells are also present in the spleen and bone marrow,[20] organs that perform critical functions in systemic iron metabolism due to the presence of CD163$^+$ iron-recycling RPMs and erythroblastic island macrophages, respectively. Therefore, we sought to accurately compare the Hb-scavenging capacity of endothelial and macrophage populations from the spleen and bone marrow with that of hepatic LSECs and KCs over a wide range of Hb doses. We used 1 μg of Hb, an amount below the binding capacity of circulating haptoglobin (10-20 μg/ml plasma), an intermediate dose of 10 μg, and 100 μg (injected together with 10 mg of unlabeled Hb), which saturates the haptoglobin pool and mimics hemolytic conditions. We also injected mice with 1 ug of Hb bound to haptoglobin. Myeloid cells or ECs of the bone marrow were not capable of efficient Hb sequestration (Fig. S3A). Strikingly, we observed the extraordinary ability of LSECs to internalize Hb as compared to the other cell types analyzed as exemplified by 70-99% of Hb-positive cells depending on

the dose (Fig. 2A) and the highest intensity of the Hb signal per cell as compared to KCs, splenic ECs, or RPMs (Fig. 2B, D, F, H). The scavenging capacity of KCs and splenic ECs was gradually increased with the Hb dose, (Fig. 2C-F), whereas RPMs contributed, albeit slightly, to the Hb clearance only at the highest dose, mimicking hemolysis (Fig. 2G and H). Finally, using whole organ imaging and flow cytometry, we did not detect Hb accumulation in the aorta, lined by non-sinusoidal ECs (Fig. S3B and C). In conclusion, our data suggest that LSECs outperform other cell types in Hb clearance over a wide range of circulating Hb concentrations.

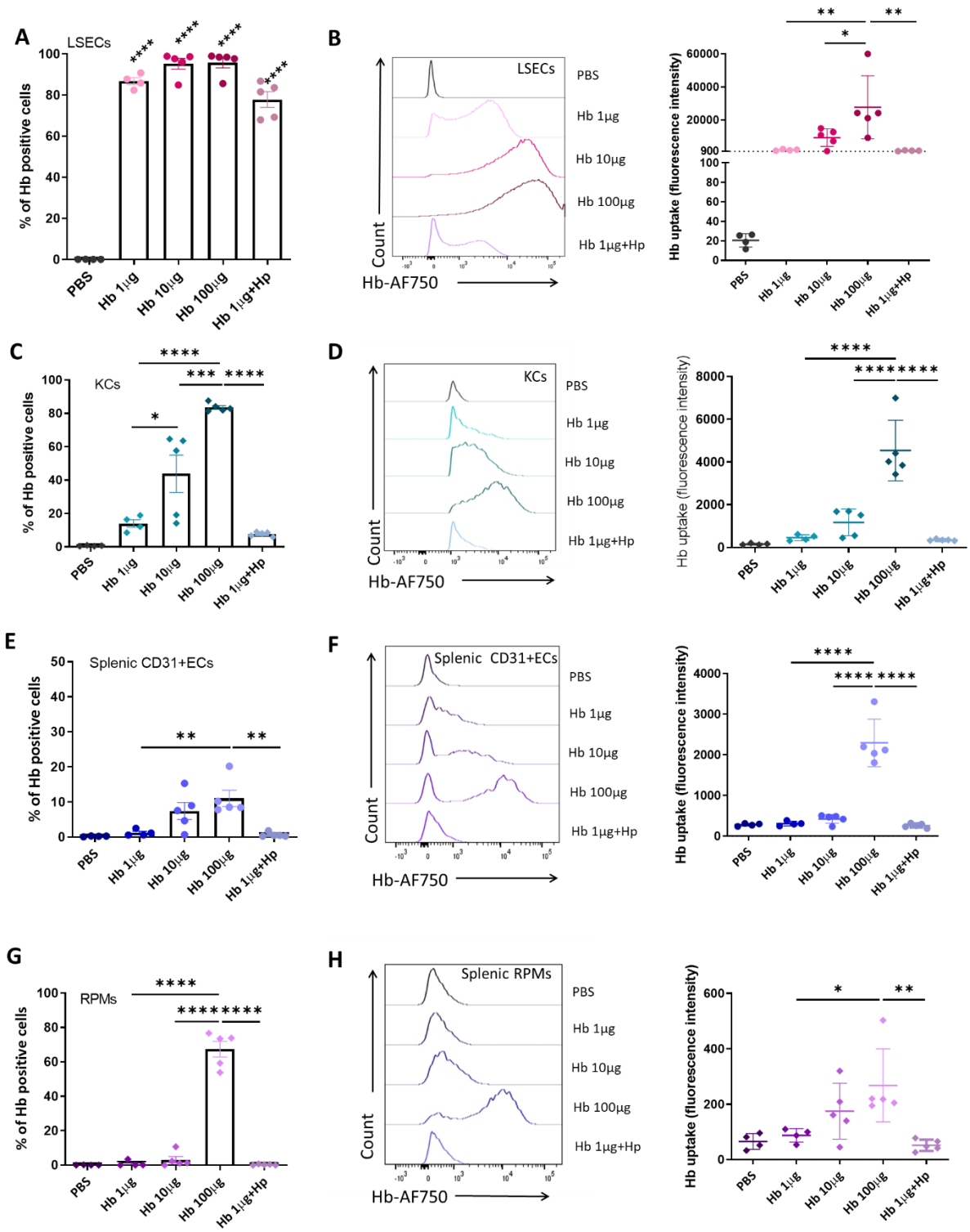

Figure 2. LSECs outperform other endothelial populations and macrophages in Hb uptake.

Percentage of Hb-AF750 uptake by (A) LSECs, (C) KCs, (E) splenic endothelial cells (ECs), and (G) RPMs. Fluorescence intensity of Hb-AF750 in (B) LSECs, (D) KCs, (F) splenic endothelial cells, and (H) RPMs. Both parameters were analyzed with flow cytometry. Data are expressed as mean ± SEM and each data point represents one biological replicate. One-way ANOVA with Tukey's Multiple Comparison tests was used to determine statistical significance; ns - not significant, *p<0.05, **p<0.01, ***p<0.001 and ****p<0.0001

LSECs constitutively express proteins critical for iron recycling from heme

We were intrigued by the fact that LSECs efficiently scavenge low doses of Hb. To further explore their specialization, we examined data from single-cell RNA sequencing of ECs from different mouse organs.[32] Interestingly, both *Hmox1* [encoding heme oxygenase 1 (HO-1)] and *Blrvb* (encoding biliverdin reductase b, BLRVB), genes important for heme catabolism, were identified as metabolic markers exclusively specific for liver EC. Using EC Atlas, we visualized the expression levels of *Hmox1* and *Blvrb*, as well as of *Slc40a1*, the gene encoding the iron exporter FPN. We found a clear signature for the high expression of these transcripts in liver ECs as compared to other organs (Fig. S4). Consistently, we detected their clear expression at the protein level in primary LSECs (Fig. 3A and B). Flow cytometric quantification revealed a significantly higher FPN expression in LSECs than in splenic and bone marrow ECs, comparable to iron-recycling KCs and RPMs, whereas HO-1 levels were intermediate between macrophages and ECs from other organs (Fig. 3C). Likewise, LSECs showed significantly higher levels of labile iron than ECs from the spleen and bone marrow (Fig. 3D). High labile iron levels in LSECs may explain why liver ECs were specifically hallmarked by high expression levels of genes essential for protection against free radicals, such as *Gpx4*, *Gclc*, and *Me2*, according to single-cell RNA sequencing.[32] FPN was robustly induced in LSECs under conditions of systemic iron deficiency caused by iron-restricted feeding (Fig. 3E), a response that mimicked that of KCs (Fig. 3F) and suggested a tight control of LSECs' FPN by circulating hepcidin. Confirming the iron-exporting function of LSEC FPN, we detected a significant increase in labile iron in LSECs in response to mini-hepcidin PR73 injection (Fig. 3G).[33] Collectively, these data indicate that LSECs are equipped with a protein machinery that drives iron recycling from heme, suggesting their role in a steady-state iron turnover.

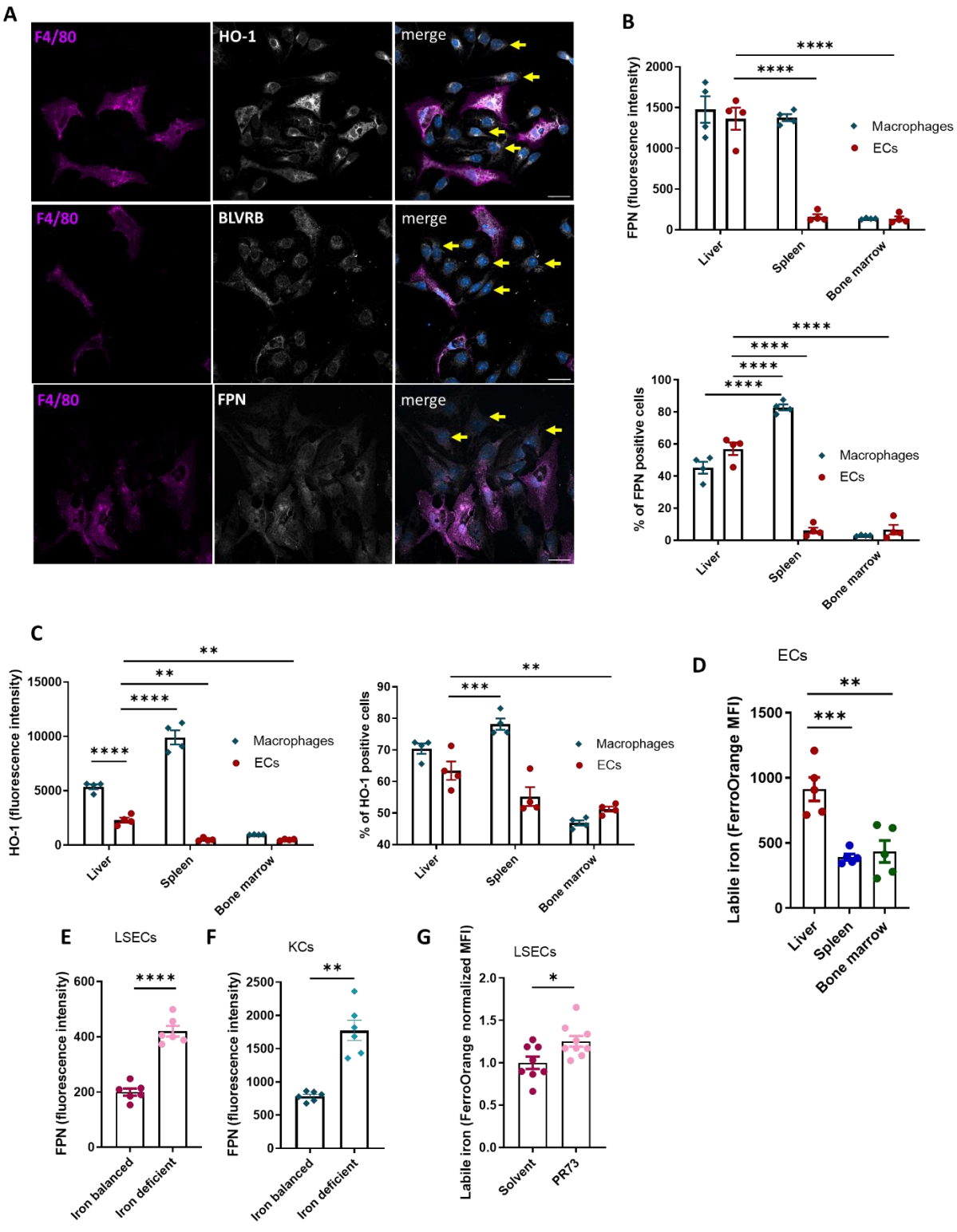

Figure 3. LSECs constitutively express proteins critical for iron recycling.

(A) HO-1, BLVRB, and FPN (white) presence in F4/80^{+} (violet) KCs and F4/80^{-} cells imaged by microscopy in NPC *in vitro* cultures. Arrows indicate non-macrophage cells positive for the respective proteins. Nuclei (blue), scale bars, 20 μm. (B-C) Flow cytometry analysis of (B) FPN and (C) HO-1 expression in macrophages and endothelial cells (ECs). (D) Cytosolic ferrous iron (Fe^{2+}) content in endothelial cells was measured with a FerroOrange probe. (E-F) Flow cytometry analysis of FPN

expression of (E) LSEC and (F) KC populations isolated from mice kept on balanced or iron-deficient diets. (G) Cytosolic ferrous iron (Fe^{2+}) content was measured with a FerroOrange probe in LSECs derived from mice injected with mini hepcidin (PR73). Microscopic images were acquired using a confocal microscope LSM 800 (Zeiss) equipped with an EC Plan-Neofluar 40x/1.30 Oil DIC M27 oil objective and T-PMT detectors. Acquisition software: ZEN 2.6. The images were processed using ImageJ software with linear gamma adjustments of contrast and brightness. Numerical data are expressed as mean ±SEM and each data point represents one biological replicate. Welch's unpaired t-test was used to determine statistical significance in E, F and G; one-way ANOVA with Tukey's Multiple Comparison tests was used in D; while two-way ANOVA with Tukey's Multiple Comparison tests was used in B and C; ns - not significant, *p<0.05, **p<0.01, ***p<0.001 and ****p<0.0001.

LSECs and KCs support iron recycling by removing hemolysis products from the spleen

We next sought to understand how LSECs might be involved in physiological iron recycling. The hemolysis-driven iron recycling model proposed by Klei et al. implied that RPMs likely sequester spleen-derived Hb via highly-expressed CD163.[5] However, CD163 knock-out mice do not show major differences in systemic and splenic iron parameters (Fig. S5). We hypothesized that hepatic cells may play a role in the clearance of splenic hemolytic products via portal circulation. We, therefore, extended previously reported studies by quantifying the contributions of splenic and hepatic myeloid and endothelial cells to the uptake of intact RBCs, RBCs devoid of cytoplasm (so-called RBC ghosts), and free Hb. To this end, we injected mice with temperature-stressed RBCs, derived from Ubi-GFP transgenic mice and stained with the membrane label PKH26 (Fig. 4A and B). This approach revealed that RPMs outperformed other splenic cell types, F4/80^{high} CD11b^{high} pre-RPMs, CD11c^{+} dendritic cells (DCs), monocytes, and splenic ECs in the sequestration of PKH26^{+}GFP^{+} intact RBCs. An equal percentage of RPMs (approximately 30% of the population) were effective in removing PKH26^{+}GFP^{-} RBC ghosts, a function that was efficiently supported by splenic pre-RPMs, and to a lesser extent by DCs, monocytes, or ECs. Interestingly, we found that in the liver phagocytosis of intact RBCs by KCs was less efficient than the uptake of RBC ghosts (Fig. 4B). No erythrophagocytosis of intact RBCs was detected in hepatic DCs and LSECs, but they showed some capacity for the sequestration of RBC membranes, albeit lower than KCs. Injection of fluorescently-labeled RBC ghosts along with free Hb confirmed that KCs and LSECs, respectively, rather than RPMs or splenic ECs, are specialized in the clearance of these two major hemolysis products (Fig. 4C and D). Consistent with these data, we detected an increase in heme levels in the portal vein plasma, but not in the systemic circulation, after injection of stressed RBCs compared to control PBS-injected mice (Fig. 4E). We next sought to determine whether the activity of LSECs to sequester Hb could be modulated by the altered capacity of splenic RPMs to fully execute

erythrophagocytosis. First, we observed that LSECs became more effective at Hb uptake in response to macrophage depletion after clodronate injection (Fig. 4F). Second, we took advantage of the physiological difference in iron parameters between BALB/C and C57BL/6J (BL/6J) mice. We observed that the lower erythrophagocytic capacity of RPMs from BALB/C mice compared to BL/6J mice (Fig. 4G), which was associated with reduced RPM FPN expression (Fig. 4H), heme accumulation in the extracellular space of the spleen and portal plasma (Fig. 4I and J), was coupled with higher levels of labile iron and greater FPN expression in LSECs (Fig. 4K and L), indicating their higher activity in iron-recycling from Hb. Taken together, our findings support a physiological role for LSECs in the sequestration of endogenous spleen-derived Hb, thereby establishing a spleen-liver axis for effective iron recycling from senescent RBCs.

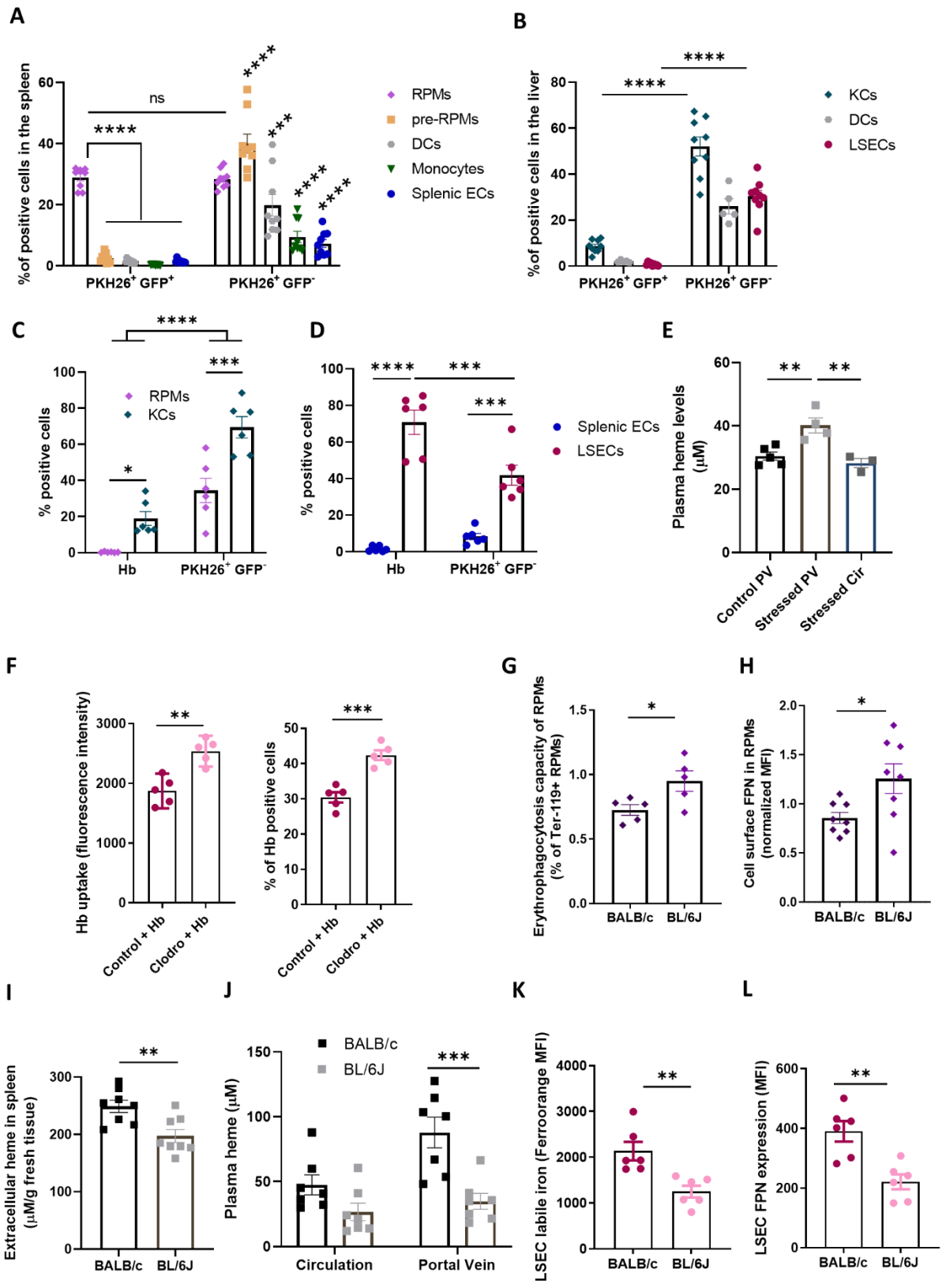

Figure 4. LSECs and KCs support iron recycling by removing hemolysis products from the spleen.

(A-D) Mice were administered i.v. with (A-B) stressed GFP$^+$ RBCs stained with a membrane marker PKH26 or (C-D) Hb-AF750 and PKH26$^+$ RBCs devoid of cytoplasm (RBC ghosts). Splenic and liver cells were isolated, stained, and analyzed by flow cytometry. (A) The percentage of cells positive for

markers of intact RBCs ($PKH26^+GFP^+$) and RBC ghosts ($PKH26^+GFP^-$) in splenic RPMs, pre-RPMs, dendritic cells (DCs), monocytes, and endothelial cells (ECs). (B) The percentage of $PKH26^+GFP^+$ and $PKH26^+GFP^-$ cells in liver KCs, dendritic cells (DCs), and LSECs. (C-D) The percentage of cells positive for Hb (AF750) and RBC ghosts. (E) Heme levels from the portal vein (PV) or circulation (Cir) plasma of control and mice transfused with temperature-stressed RBCs (sRBCs), measured by Heme Assay Kit. (F) Hb-AF750 uptake by LSECs derived from control and macrophage-depleted mice (Clodro). (G-L) BALB/c and C57BL/6J (BL/BJ) mice phenotype comparison. (G) The capacity of endogenous erythrophagocytosis assessed by intracellular staining of the erythrocytic marker (Ter-119) in RPMs. (H) FPN surface levels in RPMs measured by flow cytometry. (I) Extracellular heme content in the spleen and (J) heme levels in the portal vein and circulation plasma were measured with Heme Assay Kit. (K) Cytosolic ferrous iron (Fe^{2+}) levels in LSECs were measured with a FerroOrange probe. (L) FPN levels in LSECs measured by flow cytometry. Data are expressed as mean ± SEM and each data point represents one biological replicate. Welch's unpaired t-test was used to determine statistical significance in F-I and K-L one-way ANOVA with Tukey's Multiple Comparison tests was used in E; while two-way ANOVA with Tukey's Multiple Comparison tests was used in A-D and J; ns - not significant, *p<0.05, **p<0.01, ***p<0.001 and ****p<0.0001.

LSECs detoxify hemoglobin upon hemolysis and trigger the iron-sensing BMP6 angiokine

We next set out to investigate the response of LSECs to hemolytic conditions. To this end, we first injected mice with 10 mg of mouse hemoglobin (equivalent to the RBC fraction in approximately 100 µl of blood) in a time-course manner. We observed a transient increase in iron levels in the liver, but not in the spleen, which was normalized by the 24-hour endpoint (Fig. 5A and S6A). Notably, the kidney also accumulated iron that could not be mobilized and remained elevated throughout the experiment (Fig. S6B). Hemoglobin clearance in the liver resulted in a strong transcriptional induction of the heme catabolizing enzyme *Hmox1*, a response that could be attributed specifically to LSECs (Fig. 5B and C). It also significantly increased the number of LSECs expressing FPN on the cell surface (Fig. 5D). Hemoglobin challenge rapidly increased the expression of the iron-sensing gene *Bmp6* in FACS-sorted LSECs, accompanied by the upregulation of the BMP target gene hepcidin (*Hamp*) in the liver, (Fig. 5E-G). As expected, induction of the BMP6-hepcidin axis caused serum hypoferremia at the 15 h time point which also normalized after 24 h (Fig. 5H), reflecting the changes in liver iron content (Fig. 5A). The rapid induction of *Hmox1* in LSECs upon intravenous Hb delivery was phenocopied by injecting the mice with the hemolytic agent phenylhydrazine (PHZ) and exceeded by far the response of KCs, splenic cells and aorta (Fig. 5I and J). PHZ also caused a significant, albeit mild, iron accumulation in the liver (Fig. 5K), but not in other organs (Fig. S6C and D), and activation of *Bmp6* transcription (Fig. 5L).

Finally, we aimed to determine whether LSECs induce a specific response when exposed to Hb compared to non-heme iron. To this end, we performed RNA sequencing to assess global gene expression signatures upon injection of 10 mg of Hb and a quantitatively adjusted dose of iron

citrate. Although both stimuli elicited a very similar induction of *Bmp6*, they elicited different responses of LSECs at the transcriptome-wide level (Fig. 5M). While only 64 genes, mainly attributable to the response to oxidative stress and iron were co-induced by Hb and iron citrate (Fig. 5M), as many as 372 and 202 genes up-regulated their expression specifically upon Hb and iron citrate injection, respectively. These differences were reflected by a largely distinct functional enrichment within the Hb- and iron-induced transcriptional signature (Fig. 5N). Interestingly, Hb-exposed LSECs specifically induced genes associated with immune and inflammatory responses, such as the phagocyte marker *Cd68*, the chemokines *Ccl24*, *Ccl6*, and *Ccl9*, and importantly, *Il18*, a cytokine implicated in the pathogenesis of the hemolytic sickle cell disease.[34] Furthermore, Hb ingestion activated gene expression signatures associated with phagocytosis, the PI3K-Akt pathway, growth factor activity, and intracellular signaling, enriched categories with several links to actin remodeling and, in some cases, directly to macropinocytosis. Indeed, several genes induced by Hb, such as the receptors *Axl*, *Csf1r*, and *Met*, the growth factors *Hgf* and *Pdgfa*, or the actin cytoskeleton-interacting factors *Evl* and *Coro1a* are known to play a role in the regulation and/or execution of macropinocytosis.[27,35-37] Collectively, these findings support the role of LSECs in Hb clearance and demonstrate their high capacity to trigger the iron-sensing *Bmp6* angiokine in response to excessive Hb, along with specific pro-inflammatory markers and factors associated with actin remodeling.

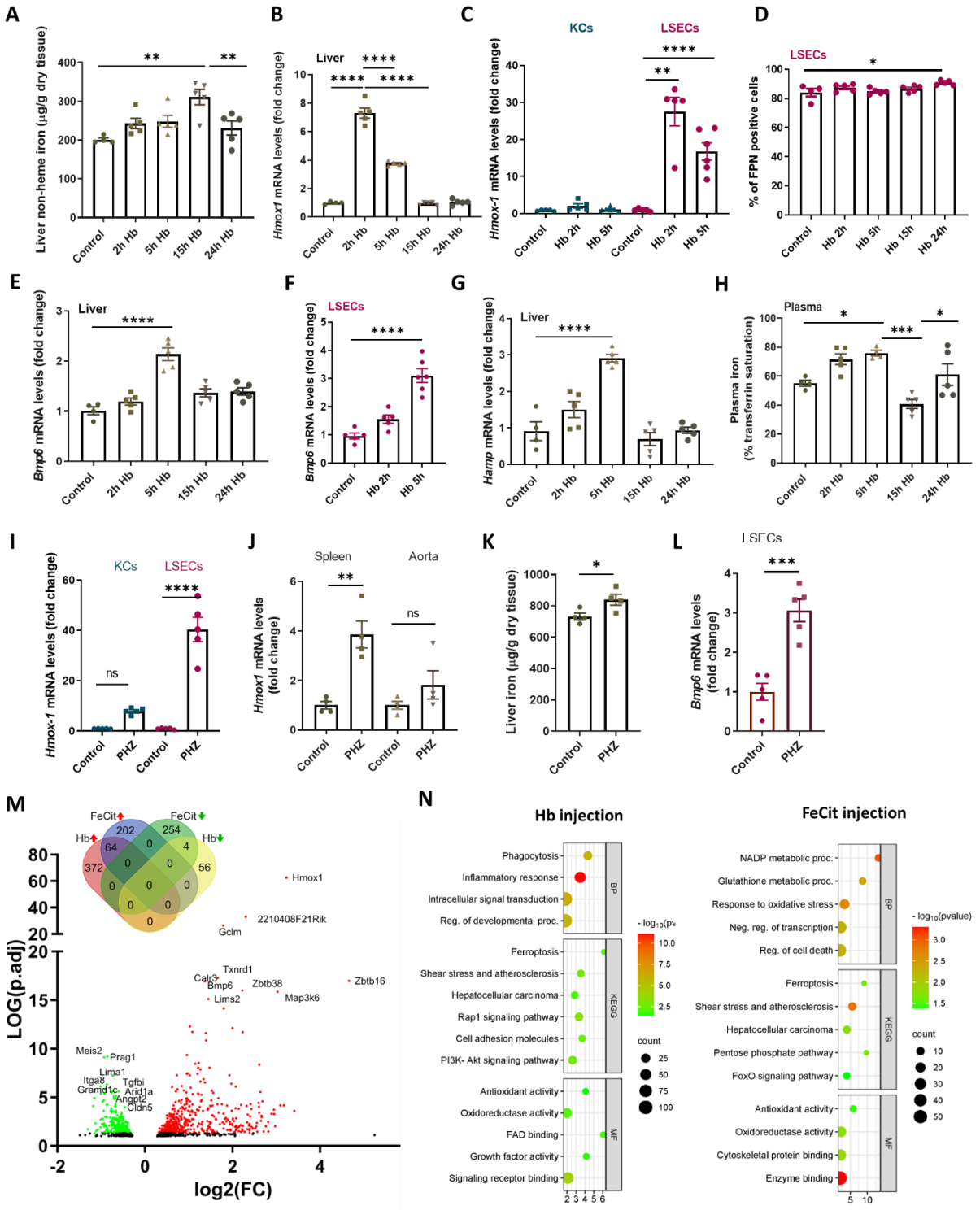

Figure 5. LSECs detoxify hemoglobin upon hemolysis and trigger the iron-sensing BMP6 angiokine.

(A-G) Mice were injected with native hemoglobin (Hb, 10 mg/mouse) and analyzed at indicated time points. (A) Non-heme iron content in the liver was measured by bathophenanthroline colorimetric assay. (B and C) *Hmox1* gene expression measurement by RT-PCR in (B) the liver and (C) FACS-sorted KC and LSEC populations. (D) FPN levels in LSECs were measured with flow cytometry. (E, F) *Bmp6* and (G) *Hamp* gene expression measured by RT-qPCR in whole livers or sorted LSECs, as indicated. (H)

Plasma iron levels were determined by transferrin saturation measurements. (I-L) Hemolysis was induced in mice by i.p. injection of phenylhydrazine (PHZ, 0.125 mg/g) 6 h before analysis. *Hmox1* gene expression in (I) FACS-sorted cell populations of KCs and LSECs, and (J) spleen and aorta. (K) Non-heme iron content in the liver. (L) *Bmp6* expression in FACS-sorted LSECs. Data are expressed as mean ± SEM and each data point represents one biological replicate. (M-N) Mice were injected with Hb (10 mg) or Ferric citrate (FeCit, 150 μg) for 5 h. (M) A volcano plot of differentially regulated genes identified by the RNASeq transcriptomic analysis in FACS-sorted LSECs. The green color indicates negatively, and the red color positively regulated genes. Venn diagram shows genes regulated by Hb and FeCit. (N) functional enrichment among genes induced by Hb or FeCit. The x-axis represents the fold of enrichment. The y-axis represents GO terms of biological processes (BP), Kyoto Encyclopedia of Genes and Genomes terms (KEGG), and GO terms of molecular function (MF). The size of the dot represents the number of genes under a specific term. The color of the dots represents the adjusted P-value. Welch's unpaired t-test was used to determine statistical significance in K-L, one-way ANOVA with Tukey's Multiple Comparison tests was used in A-B and, D-H; while two-way ANOVA with Tukey's Multiple Comparison tests was used in C, I and J; ns - not significant, *p<0.05, **p<0.01, ***p<0.001 and ****p<0.0001.

Discussion

Recent advances have revealed the critical role of the specialized hepatic sinusoidal endothelium in maintaining systemic and liver homeostasis. The scavenging activity of LSECs is essential for the hepatic clearance of biological macromolecules, such as denatured collagen, glycans/glycation end products, modified low-density lipoproteins, small immune complexes, lipopolysaccharides or viruses.[20,21,38-40] In addition, LSECs regulate the vascular tone in the liver, balance the tolerogenic immune milieu with the onset of immune responses, ensure physiological zonation of hepatic immune cells,[40,41] and control iron balance by producing the angiokines BMP2 and BMP6.[22,23] Our study identifies the novel homeostatic role of LSECs in the clearance of free Hb, an activity that converges with their scavenging and iron-regulatory functions.

The clearance functions of LSECs have been attributed to their extraordinary endocytic activity and the surface expression of scavenger receptors.[20] We discovered that LSECs have a remarkable and constitutive capacity for macropinocytosis, similar to that of macrophages, which use this pathway for antigen presentation, and in contrast to the inducible macropinocytosis of cancer cells, which is critical for nutrient acquisition.[26,28] We show that this capability distinguishes LSECs from ECs of other organs, thus significantly expanding the scarce knowledge on the macropinocytic activity of ECs[42] and assigning physiological significance to early observations that LSECs can engage macropinocytosis for antigen capture.[43] We propose that macropinocytosis of LSECs likely contributes to their scavenging function. While this possibility merits future studies, macropinocytosis has recently been

identified as a major driver of LDL uptake by macrophages, leading to foam cell formation in atherosclerosis.[44] Hence, our findings aid in shifting the paradigm from the sole role of scavenger receptor-mediated endocytosis in the clearance of blood-borne macromolecules, emphasizing the importance of macropinocytic uptake. Further studies would be required to address mechanistic details of how β-catenin signaling supports macropinocytosis of LSECs and whether its pharmacological blockade would impair liver clearance functions.

Our study employed *in vivo* approaches to verify the role of macrophages in Hb uptake and revealed that LSECs qualitatively and quantitatively outcompete CD163-expressing KCs and RPMs in this task. These provocative findings may be explained by the fact that the role of CD163 in Hb uptake has been mainly investigated by its ectopic expression in non-macrophage cells and by using polyclonal blocking anti-CD163 in cultured macrophages.[9,11,45] Our study does not exclude the contribution of iron-recycling macrophages to Hb uptake in hemolytic conditions, nor does it imply that other tissues/endothelial cells are unaffected by prolonged and pathological exposure to free Hb and heme.[46] It remains to be determined to what extent LSEC-mediated Hb uptake protects other organs in hemolytic disorders, such as sickle cell disease or thalassemia, and whether and how LSEC functions are impaired in such conditions. Noteworthy, CD163-expressing macrophages play important anti-inflammatory roles, for example in the tumor microenvironment or arthritis, but these tissue-specific roles do not appear to be related to Hb clearance.[47-49] Finally, even though the clearance of free circulating Hb was much faster than that of Hb-haptoglobin complexes in dogs,[10] consistent with our model, the CD163-independent uptake of Hb by LSECs would need to be verified in human cells.

Most importantly, our study defines and quantifies the individual contribution of splenic and hepatic cell types to physiological iron recycling. Consistent with previous studies,[3,4] we provide evidence that RPMs are efficient at phagocytosis of intact stressed RBCs, whereas the liver is the site of scavenging steady-state hemolytic products. KCs are efficient in the uptake of RBC ghosts and outperform RPMs in the Hb uptake. LSECs, due to their anatomical location, exceptional macropinocytic activity, and expression of the iron-recycling proteins, emerge as a novel cell type involved in the maintenance of iron homeostasis, specialized for the removal of spleen-derived Hb. Consistent with this newly proposed role of LSECs, it has been reported that endothelial-specific FPN knock-out mice exhibit marked iron deficiency, develop anemia, and show iron loading in liver NPC.[50] Further studies using cell-type specific genetic deletions of proteins involved in iron recycling would be crucial to quantify the exact contribution of

RPMs, KCs, and LSECs to the circulating plasma iron pool and thus assess their relative involvement in iron recycling from RBCs.

Methods

Mice and *in vivo* procedures

Female BALB/c mice (8-10 weeks old) were obtained from the Experimental Medicine Centre of the Medical University of Bialystok or the Mossakowski Medical Research Institute of the Polish Academy of Sciences. Female C57BL/6-Tg(UBC-GFP)30Scha/J (UBI-GFP/BL6) mice were kindly provided by Aneta Suwińska (Faculty of Biology, University of Warsaw, Poland). Female and male (8-12 weeks old) WT C57BL/6J and *Cd163*$^{-/-}$ mice were kindly provided by Anders Etzerodt (Department of Biomedicine, Aarhus University, Denmark). For the dietary experiment, C57BL/6J females (4 weeks old) were obtained from the Experimental Medicine Centre of the Medical University of Bialystok. Mice were fed with a standard iron diet of 200 mg/kg (control) or a low iron diet containing <6 mg/kg (iron deficient) for 5 weeks before analysis. All mice were maintained at the SPF facility under standard conditions (20°C, humidity 60%, 12-h light/dark cycle). All animal experiments were conducted following the guidelines of European Directive 2010/63/EU and the Federation for Laboratory Animal Science Associations. The procedures were approved by the local ethical committee in Warsaw (No. WAW2/150/2019, WAW2/138/2019, WAW2/137/2020, WAW2/137/2021, WAW2/179/2021, and WAW2/094/2021), or for the dietary experiment by the local ethical committee in Olsztyn No. 26/2018.

Proteins or their conjugates were dissolved in PBS and administered intravenously (*i.v.*) at the dose indicated in the particular figure legend. For macrophage depletion, mice received *i.v.*solution of liposomes containing clodronic acid (LIPOSOMA, #C-SUV-005) (5 ml/kg) or control empty liposomes for 24 h. A sterile aqueous iron citrate (FeCit, 150 µg/mouse) solution (Sigma-Aldrich-Aldrich, #F3388) or sterile citric acid buffer (0.05 M, Sigma-Aldrich, #251275) were normalized to pH 7.0 and administered *i.v.* for 5 h. Mini-hepcidin (PR73, 50 nmol/mouse) (kind gift from Elizabeta Nemeth, UCLA, USA) was injected intraperitoneally (*i.p.*) for 4 h. To induce hemolysis, a sterile solution of phenylhydrazine (PHZ) (Sigma-Aldrich, #P26252) in PBS was administered *i.p.* at a dose of 0.125 mg/g of body weight for 6 h. PKH26-stained (Sigma Aldrich, #PKH26GL-1KT) temperature-stressed UBI-GFP RBCs were resuspended to 50% hematocrit in HBSS (Capricorn, #HBSS-1A) and administered *i.v.* for

1.5 h. PKH26-stained RBCs ghosts were mixed with fluorescently labeled Hb (10 μg/mouse) and administered *i.v.*for 1.5 h.

Cell-based and biochemical assays

Isolation of non-parenchymal liver cells (NPCs) for primary cell cultures together with cell treatments and immunofluorescence are described in the Supplementary Methods. Isolation of cells from the spleen, bone marrow, and aorta, flow cytometry, FACS-sorting, liver tissue immunofluorescence, heme/iron measurements, preparation of conjugated mouse Hb, stressed RBCs, and RBC ghosts, and real-time quantitative PCR (RT-qPCR) were performed as previously reported,[25] or/and described in detail in Supplementary Methods.

RNA sequencing

Transcriptome analysis of LSECs was conducted using the AmpliSeq method as described in the Supplementary Methods. Data for iron citrate injection were deposited previously in the GEO repository under accession no GSE235976 (secured with a token: ubcbegoyrxglfeb to allow review), whereas for Hb injection under no GSE240270 (with a token: uhkrgywyhledjmj).

Acknowledgments

This work was funded by the National Science Centre grant 2018/31/B/NZ4/03676 to KMS and the Foundation of Polish Science grant TEAM TECH/2016-1/8 to TPR. We express gratitude to Marta Niklewicz for her substantial technical assistance in this project. We would like to thank Daria Zdżalik-Bielecka for her valuable advice during the initial phases of the project, and to Rafał Mazgaj for providing technical assistance in conducting experiments with confocal microscopy. Additionally, we extend our thanks to Damian Strzemecki for his technical assistance in performing mice injections. We thank Tara Arvedson (Amgen Inc. USA) for the anti-ferroportin antibody, Elizabeta Nemeth for PR73, and Aneta Suwińska for sharing UBI-GFP/BL6 mice. Many thanks to Agnieszka Popielska and Anna Kosson, and the staff of the Experimental Medicine Centre (Bialystok, Poland) and Mossakowski Medical Research Institute (Warsaw, Poland) for their technical support.

Authorship Contributions

KMS, GZ, TPR, ZS, and MMio conceived and planned the experiments; ZS, GZ, AJ, PS, RM, MC, IR, KJ, and MMo performed research; GZ, ZS, AJ, PS, RM, MC, MK, analyzed data; GZ, ZS, AJ, PS, RM, MC, KJ, KMS, MMik, visualized data; MMik curated RNA-Seq data; KMS,

TPR supervised the study; TPR, AJ, MMio and AE edited the manuscript; KMS, GZ, and ZS wrote the manuscript.

Conflict of Interest Disclosure

The authors declare that they have no conflict of interest.

References

1. Slusarczyk P, Mleczko-Sanecka K. The Multiple Facets of Iron Recycling. *Genes (Basel)*. 2021;12(9).
2. Muckenthaler MU, Rivella S, Hentze MW, Galy B. A Red Carpet for Iron Metabolism. *Cell*. 2017;168(3):344-361.
3. Youssef LA, Rebbaa A, Pampou S, et al. Increased erythrophagocytosis induces ferroptosis in red pulp macrophages in a mouse model of transfusion. *Blood*. 2018;131(23):2581-2593.
4. Ma S, Dubin AE, Zhang Y, et al. A role of PIEZO1 in iron metabolism in mice and humans. *Cell*. 2021;184(4):969-982 e913.
5. Klei TRL, Dalimot J, Nota B, et al. Hemolysis in the spleen drives erythrocyte turnover. *Blood*. 2020;136(14):1579-1589.
6. Kato GJ, Steinberg MH, Gladwin MT. Intravascular hemolysis and the pathophysiology of sickle cell disease. *J Clin Invest*. 2017;127(3):750-760.
7. Schaer DJ, Vinchi F, Ingoglia G, Tolosano E, Buehler PW. Haptoglobin, hemopexin, and related defense pathways-basic science, clinical perspectives, and drug development. *Front Physiol*. 2014;5:415.
8. Wang Y, Kinzie E, Berger FG, Lim SK, Baumann H. Haptoglobin, an inflammation-inducible plasma protein. *Redox Rep*. 2001;6(6):379-385.
9. Kristiansen M, Graversen JH, Jacobsen C, et al. Identification of the haemoglobin scavenger receptor. *Nature*. 2001;409(6817):198-201.
10. Boretti FS, Baek JH, Palmer AF, Schaer DJ, Buehler PW. Modeling hemoglobin and hemoglobin:haptoglobin complex clearance in a non-rodent species-pharmacokinetic and therapeutic implications. *Front Physiol*. 2014;5:385.
11. Schaer DJ, Schaer CA, Buehler PW, et al. CD163 is the macrophage scavenger receptor for native and chemically modified hemoglobins in the absence of haptoglobin. *Blood*. 2006;107(1):373-380.

12. Etzerodt A, Kjolby M, Nielsen MJ, Maniecki M, Svendsen P, Moestrup SK. Plasma clearance of hemoglobin and haptoglobin in mice and effect of CD163 gene targeting disruption. *Antioxid Redox Signal.* 2013;18(17):2254-2263.
13. Theurl I, Hilgendorf I, Nairz M, et al. On-demand erythrocyte disposal and iron recycling requires transient macrophages in the liver. *Nat Med.* 2016;22(8):945-951.
14. Vinchi F, De Franceschi L, Ghigo A, et al. Hemopexin therapy improves cardiovascular function by preventing heme-induced endothelial toxicity in mouse models of hemolytic diseases. *Circulation.* 2013;127(12):1317-1329.
15. Vinchi F, Sparla R, Passos ST, et al. Vasculo-toxic and pro-inflammatory action of unbound haemoglobin, haem and iron in transfusion-dependent patients with haemolytic anaemias. *Br J Haematol.* 2021;193(3):637-658.
16. Fagoonee S, Gburek J, Hirsch E, et al. Plasma protein haptoglobin modulates renal iron loading. *Am J Pathol.* 2005;166(4):973-983.
17. Marro S, Barisani D, Chiabrando D, et al. Lack of haptoglobin affects iron transport across duodenum by modulating ferroportin expression. *Gastroenterology.* 2007;133(4):1261-1271.
18. Poisson J, Lemoinne S, Boulanger C, et al. Liver sinusoidal endothelial cells: Physiology and role in liver diseases. *Journal of hepatology.* 2017;66(1):212-227.
19. Sorensen KK, McCourt P, Berg T, et al. The scavenger endothelial cell: a new player in homeostasis and immunity. *American journal of physiology Regulatory, integrative and comparative physiology.* 2012;303(12):R1217-1230.
20. Koch PS, Lee KH, Goerdt S, Augustin HG. Angiodiversity and organotypic functions of sinusoidal endothelial cells. *Angiogenesis.* 2021;24(2):289-310.
21. Schledzewski K, Geraud C, Arnold B, et al. Deficiency of liver sinusoidal scavenger receptors stabilin-1 and -2 in mice causes glomerulofibrotic nephropathy via impaired hepatic clearance of noxious blood factors. *J Clin Invest.* 2011;121(2):703-714.
22. Koch PS, Olsavszky V, Ulbrich F, et al. Angiocrine Bmp2 signaling in murine liver controls normal iron homeostasis. *Blood.* 2017;129(4):415-419.
23. Canali S, Zumbrennen-Bullough KB, Core AB, et al. Endothelial cells produce bone morphogenetic protein 6 required for iron homeostasis in mice. *Blood.* 2017;129(4):405-414.
24. Mleczko-Sanecka K, Silvestri L. Cell-type-specific insights into iron regulatory processes. *Am J Hematol.* 2021;96(1):110-127.

25. Slusarczyk P, Mandal PK, Zurawska G, et al. Impaired iron recycling from erythrocytes is an early hallmark of aging. *Elife.* 2023;12.
26. Canton J. Macropinocytosis: New Insights Into Its Underappreciated Role in Innate Immune Cell Surveillance. *Front Immunol.* 2018;9:2286.
27. Zdzalik-Bielecka D, Poswiata A, Kozik K, et al. The GAS6-AXL signaling pathway triggers actin remodeling that drives membrane ruffling, macropinocytosis, and cancer-cell invasion. *Proc Natl Acad Sci U S A.* 2021;118(28).
28. Commisso C, Davidson SM, Soydaner-Azeloglu RG, et al. Macropinocytosis of protein is an amino acid supply route in Ras-transformed cells. *Nature.* 2013;497(7451):633-637.
29. Klein D, Demory A, Peyre F, et al. Wnt2 acts as a cell type-specific, autocrine growth factor in rat hepatic sinusoidal endothelial cells cross-stimulating the VEGF pathway. *Hepatology.* 2008;47(3):1018-1031.
30. Tejeda-Munoz N, Albrecht LV, Bui MH, De Robertis EM. Wnt canonical pathway activates macropinocytosis and lysosomal degradation of extracellular proteins. *Proc Natl Acad Sci U S A.* 2019;116(21):10402-10411.
31. Redelman-Sidi G, Binyamin A, Gaeta I, et al. The Canonical Wnt Pathway Drives Macropinocytosis in Cancer. *Cancer Res.* 2018;78(16):4658-4670.
32. Kalucka J, de Rooij L, Goveia J, et al. Single-Cell Transcriptome Atlas of Murine Endothelial Cells. *Cell.* 2020;180(4):764-779 e720.
33. Stefanova D, Raychev A, Deville J, et al. Hepcidin Protects against Lethal Escherichia coli Sepsis in Mice Inoculated with Isolates from Septic Patients. *Infect Immun.* 2018;86(7).
34. Gupta A, Fei YD, Kim TY, et al. IL-18 mediates sickle cell cardiomyopathy and ventricular arrhythmias. *Blood.* 2021;137(9):1208-1218.
35. BoseDasgupta S, Moes S, Jenoe P, Pieters J. Cytokine-induced macropinocytosis in macrophages is regulated by 14-3-3zeta through its interaction with serine-phosphorylated coronin 1. *FEBS J.* 2015;282(7):1167-1181.
36. Visweshwaran SP, Nayab H, Hoffmann L, et al. Ena/VASP proteins at the crossroads of actin nucleation pathways in dendritic cell migration. *Front Cell Dev Biol.* 2022;10:1008898.
37. Recouvreux MV, Commisso C. Macropinocytosis: A Metabolic Adaptation to Nutrient Stress in Cancer. *Front Endocrinol (Lausanne).* 2017;8:261.

575 38. Ganesan LP, Kim J, Wu Y, et al. FcgammaRIIb on liver sinusoidal endothelium clears
576 small immune complexes. *J Immunol.* 2012;189(10):4981-4988.
577 39. Malovic I, Sorensen KK, Elvevold KH, et al. The mannose receptor on murine liver
578 sinusoidal endothelial cells is the main denatured collagen clearance receptor.
579 *Hepatology.* 2007;45(6):1454-1461.
580 40. Shetty S, Lalor PF, Adams DH. Liver sinusoidal endothelial cells - gatekeepers of
581 hepatic immunity. *Nat Rev Gastroenterol Hepatol.* 2018;15(9):555-567.
582 41. Gola A, Dorrington MG, Speranza E, et al. Commensal-driven immune zonation of the
583 liver promotes host defence. *Nature.* 2021;589(7840):131-136.
584 42. Lin XP, Mintern JD, Gleeson PA. Macropinocytosis in Different Cell Types:
585 Similarities and Differences. *Membranes (Basel).* 2020;10(8).
586 43. Connolly MK, Bedrosian AS, Malhotra A, et al. In hepatic fibrosis, liver sinusoidal
587 endothelial cells acquire enhanced immunogenicity. *J Immunol.* 2010;185(4):2200-
588 2208.
589 44. Lin HP, Singla B, Ahn W, et al. Receptor-independent fluid-phase macropinocytosis
590 promotes arterial foam cell formation and atherosclerosis. *Sci Transl Med.*
591 2022;14(663):eadd2376.
592 45. Schaer CA, Schoedon G, Imhof A, Kurrer MO, Schaer DJ. Constitutive endocytosis of
593 CD163 mediates hemoglobin-heme uptake and determines the noninflammatory and
594 protective transcriptional response of macrophages to hemoglobin. *Circ Res.*
595 2006;99(9):943-950.
596 46. Buehler PW, Humar R, Schaer DJ. Haptoglobin Therapeutics and
597 Compartmentalization of Cell-Free Hemoglobin Toxicity. *Trends Mol Med.*
598 2020;26(7):683-697.
599 47. Etzerodt A, Tsalkitzi K, Maniecki M, et al. Specific targeting of CD163(+) TAMs
600 mobilizes inflammatory monocytes and promotes T cell-mediated tumor regression. *J*
601 *Exp Med.* 2019;216(10):2394-2411.
602 48. Etzerodt A, Moulin M, Doktor TK, et al. Tissue-resident macrophages in omentum
603 promote metastatic spread of ovarian cancer. *J Exp Med.* 2020;217(4).
604 49. Svendsen P, Etzerodt A, Deleuran BW, Moestrup SK. Mouse CD163 deficiency
605 strongly enhances experimental collagen-induced arthritis. *Sci Rep.* 2020;10(1):12447.
606 50. Zhang Z, Guo X, Herrera C, et al. Bmp6 expression can be regulated independently of
607 liver iron in mice. *PLoS One.* 2014;9(1):e84906.